The Journal of Veterinary Medical Science

FULL PAPER

Pathology

Pathological lesions in the central nervous system and peripheral tissues of *dd*Y mice with street rabies virus (1088 strain)

Kazunori KIMITSUKI[1)], Kentaro YAMADA[2)], Nozomi SHIWA[1)], Satoshi INOUE[3)], Akira NISHIZONO[2, 4)] and Chun-Ho PARK[1)]*

[1)]Department of Veterinary Pathology, School of Veterinary Medicine, Kitasato University, 23-35-1, Higashi, Towada, Aomori 034-8628, Japan
[2)]Research Promotion Project, Oita University, 1-1 Idaigaoka, Hasama-machi, Yufu, Oita 879-5593, Japan
[3)]Department of Veterinary Science, National Institute of Infectious Diseases, Toyama 1-23-1, Shinjuku-ku, Tokyo 162-8640 Japan
[4)]Department of Microbiology, Faculty of Medicine, Oita University, 1-1 Idaigaoka, Hasama-machi, Yufu, Oita 879-5593, Japan

ABSTRACT. Most studies on rabies virus pathogenesis in animal models have employed fixed rabies viruses, and the results of those employing street rabies viruses have been inconsistent. Therefore, to clarify the pathogenesis of street rabies virus (1088 strain) in mice, 10^6 focus forming units were inoculated into the right hindlimb of *dd*Y mice (6 weeks, female). At 3 days postinoculation (DPI), mild inflammation was observed in the hindlimb muscle. At 5 DPI, ganglion cells in the right lumbosacral spinal dorsal root ganglia showed chromatolysis. Axonal degeneration and inflammatory cells increased with infection progress in the spinal dorsal horn and dorsal root ganglia. Right hindlimb paralysis was observed from 7 DPI, which progressed to quadriparalysis. However, no pathological changes were observed in the ventral horn and root fibers of the spinal cord. Viral antigen was first detected in the right hindlimb muscle at 3 DPI, followed by the right lumbosacral dorsal root ganglia, dorsal horn of spinal cord, left red nuclei, medulla oblongata and cerebral cortex (M1 area) at 5 DPI. These results suggested that the 1088 virus ascended the lumbosacral spinal cord via mainly afferent fibers at early stage of infection and moved to cerebral cortex (M1 area) using descending spinal tract. Additionally, we concluded that significant pathological changes in mice infected with 1088 strain occur in the sensory tract of the spinal cord; this selective susceptibility results in clinical features of the disease.

KEY WORDS: central nervous system, *dd*Y mouse, dorsal root ganglion, pathogenesis, street rabies virus (1088 strain)

J. Vet. Med. Sci.
79(6): 970–978, 2017
doi: 10.1292/jvms.17-0028

Received: 20 January 2017
Accepted: 6 April 2017
Published online in J-STAGE: 20 April 2017

Rabies virus is a neurotropic virus that causes fatal encephalomyelitis in humans and animals [11, 20, 25]. In Asia and Africa, approximately 55,000 people die annually, because of infection with rabies virus transmitted by rabid dogs [15]. Rabies viruses are generally classified into two categories, street rabies viruses and fixed viruses. Following experimental infection with street rabies viruses, central nervous system (CNS) lesions have been characterized by non-suppurative meningoencephalomyelitis with neuronal necrosis which may be accompanied with neuronophagia, focal gliosis, perivascular cuffing and Negri bodies [5, 6]. However, these features are not always presented by all street rabies virus infections. In mouse inoculation models, encephalitic changes (perivascular cuffing, apoptosis and necrosis) do not occur after infection with the highly neuro-invasive silver-haired bat rabies virus [27, 35]. Human beings, naturally infected with street rabies virus, rarely exhibit CNS inflammation; however, minimal inflammatory changes, such as increased microglial activation, may be observed with prolonged clinical illness [10]. These differences in pathogenesis among street rabies virus strains are probably associated with the mechanism of neuronal dysfunction, mode of viral spread in the brain and nature of the stimulus for inflammatory infiltration. So far, most studies on the neuropathogenesis of rabies have employed animal models using fixed viruses, because of regularity and shortening of the incubation period, stabilization of virulence and a reduction or loss of infectivity after peripheral inoculation [2, 17]. By contrast, the pathogenesis of street rabies viruses in animals is not fully understood.

Street rabies virus 1088 strain, isolated from a woodchuck in the Centers for Disease Control and Prevention in Atlanta in

*Correspondence to: Park, C.-H., Department of Veterinary Pathology, School of Veterinary Medicine, Kitasato University, 23-35-1 Higashi, Towada, Aomori 034-8628, Japan. e-mail: baku@vmas.kitasato-u.ac.jp

U.S.A., displayed strong neurotropism and resulted in mortality when intramuscularly injected in mice. *N*-glycosylation sites on G protein have been proposed to be one of the determinants of 1088 strain pathogenicity in mice [34]. However, the pathogenesis and detailed pathological findings of 1088 strain infection in mice have still not been published. Therefore, to clarify the pathogenesis of street rabies virus (1088 strain) in mice, the right hindlimb of *dd*Y mice was inoculated.

MATERIALS AND METHODS

Virus, mice and virus inoculation

Street rabies virus 1088, a strain that has been isolated from a woodchuck in the Centers for Disease Control in Atlanta in U.S.A., was obtained from the Yale Arbovirus Unit of Yale University [19]. The strain had been passaged in the brains of suckling mice only twice since the original isolation. Brains were homogenized, and the supernatant of the 10% brain homogenate was used for inoculation. The virus (10^6 focus-forming units) was inoculated into the right hindlimb (surae muscles of the right triceps) of six-week-old, female *dd*Y mice (Kyudo Co., Ltd., Saga, Japan). The inoculated mice were observed daily for neurological symptoms and 5 mice were sacrificed per day at 3, 5, 8 and 11 days post-inoculation (DPI). Three mice per group were designated as negative controls and inoculated with phosphate-buffered saline instead of the virus. All animal experiments were performed with approval from the ethics committee of Oita University (Approval number, MO10005).

Necropsy and preparation of tissue sections

Each mouse was euthanized by isoflurane an inhalational anesthetic agent, and their brain, spinal cord and muscles were sampled. Tissues and organs were fixed in 10% neutral-buffered formalin solution (Wako Pure Chemicals Industries Ltd., Wako, Osaka, Japan). Spinal cord samples were removed and fixed in 10% formalin at room temperature (RT) for 3 days and decalcified in K-CX solution (Fujisawa Pharmaceutical Co., Ltd., Osaka, Japan). Transverse sections of the lumbar (L1–6) and sacral (S1–4) vertebrae of spinal cord were prepared. A complete series of paraffin sections (3 μm thickness) were mounted on glass slides. Serial sections were subjected to hematoxylin and eosin staining, special staining (Luxol Fast Blue; LFB), immunohistochemistry and *in situ* terminal deoxynucleotidyl transferase-mediated deoxyuridine triphosphate (dUTP) nick end labeling (TUNEL) assay.

Histopathological examination

Paraffin was removed from the sections by a series of xylene and ethanol treatments. Tissue sections were rinsed in distilled water (DW) for 5 min, followed by staining with hematoxylin solution for 3 min, rinsing under running tap water for 5 min, staining with eosin solution for 5 min, rinsing with distilled water and dehydration using ethanol and xylene. The sections were then mixed with a mounting medium for microscopy. For special staining, deparaffinized sections were immersed in 0.005% acetic acid solution in 95% ethyl alcohol at room temperature for 5 min, placed in 0.1% LFB solution for 16 hr in a 60°C oven and finally rinsed in DW. Sections were immersed in 0.05% lithium carbonate solution for 20 sec and washed in DW. Sections were counterstained using cresyl violet solution for 1 min, rinsed with DW for 5 min and mounted for microscopic analysis.

Immunohistochemistry

Immunohistochemical analysis was performed as previously reported [4, 16]. For detection of rabies virus antigens and cell type in tissues, the following antibodies were used: rabbit polyclonal rabies phosphoprotein (anti-P) [29], rabbit polyclonal ionized calcium binding adaptor molecule 1 (Iba1, Wako), rabbit polyclonal glial fibrillary acidic protein (GFAP; Nichirei Biosciences Inc., Tokyo, Japan), rabbit polyclonal CD3 (Agilent Technologies, Santa Clara, CA, U.S.A.), rabbit polyclonal CD20 (Spring Biosciences, Fremont, CA, U.S.A.) and mouse monoclonal neurofilament protein (NF; Agilent Technologies). After deparaffinization, sections were treated with 0.25% trypsin at room temperature for 30 min for anti-P detection; 10 mM sodium citrate buffer (pH 6.0) in a water bath at 95°C for 30 min for Iba1 detection; 10 mM sodium citrate buffer (pH 6.0) in a microwave oven at 750 W for 5 min for detection CD20; Histofine® pH 9.0 (Nichirei Biosciences) in a microwave oven at 750 W for 5 min for CD3 detection; and Proteinase-K (Agilent Technologies) at room temperature for 30 min for NF detection. To remove endogenous peroxidase activity, tissue sections were immersed in 0.3% H_2O_2 in methanol for anti-P detection and in 3% H_2O_2 in methanol for Iba1, CD3, CD20, NF and GFAP detection. Sections were then treated with 10% normal goat serum (Nichirei Biosciences) and incubated with primary antibodies at 4°C in a humidified chamber (1:1,200 for anti-P and 1:500 for Iba1) overnight. Antibodies against GFAP were incubated at RT for 1 hr. To detect primary antibodies, Envision + System Labeled Polymer-HRP anti-rabbit antibody (Agilent Technologies), Histofine® Simple Stain™ MAX PO (Rabbit) (Nichirei Biosciences) and Histofine® Simple Stain™ MAX PO (Mouse) (Nichirei Biosciences) were used. Finally, each antigen-antibody reaction was visualized using 3, 3′-diaminobenzidine (Agilent Technologies). Slides were counterstained with hematoxylin.

Terminal deoxynucleotidyl transferase-mediated dUTP-biotin nick end labeling (TUNEL) assay

The presence of fragmented DNA was determined using TUNEL (Chemicon, Temecula, CA, U.S.A.). Deparaffinization of the sections was followed by elimination of endogenous peroxidase activity by exposure to 0.3% H_2O_2 in methanol for 30 min at RT. Then, sections were treated with 20 mg/m*l* proteinase-K in 0.1 M PBS (Agilent Technologies) for 15 min at RT to activate antibodies. After washing with PBS, sections were prepared according to the manufacturer's instructions and were counterstained with hematoxylin.

Electron microscopy

After fixation in 10% neutral-buffered formalin solution, right lumbosacral spinal dorsal root ganglion cells at 8 DPI were removed under a dissection microscope (SMZ-10, Nikon, Tokyo, Japan) and fixed in 0.5% glutaraldehyde. Samples were cut into 1 mm^3 blocks, fixed in 1% buffered osmium tetroxide and embedded in epoxy resin. Sections (70 nm) were stained with uranyl acetate and lead citrate and examined using a transmission electron microscope (H-7650, Hitachi, Tokyo, Japan).

RESULTS

Clinical signs and macroscopic findings

The mice showed mild right hindlimb paralysis at 7 DPI. As the disease progressed, the mice showed bilateral hindlimb paralysis at 8 DPI and all mice were in a moribund state at 11 DPI, whereas the control mice exhibited no clinical signs. At necropsy, macroscopic findings were not observed in infected mice throughout the experimental period.

Histopathological findings

In surae muscle fibers of the right triceps, at the site of inoculation, hyaline degeneration and mild inflammatory cell infiltrates composed of lymphocytes and neutrophils were observed at 3 DPI. The increase in inflammatory cell numbers continued with progression of the infection until 11 DPI.

At 5 DPI, degenerative ganglion cells were observed in the right lumbosacral dorsal root spinal ganglia. They had medium to large cytoplasms and were intermixed with morphologically normal ganglion cells. They showed a spectrum of pathological changes with varying degrees of nuclear eccentricity, cytoplasmic chromatolysis (Fig. 1), vacuolation and neuronophagia. Their nuclei tended to be paler, and their nucleoli were somewhat smaller and less intensely stained than the intact neurons of control mice. There was no evidence of karyorrhexis or chromatin condensation, which are characteristic of apoptosis. Interestingly, these degenerative ganglion cells gradually disappeared from the right dorsal root ganglion, and similar ganglion cells appeared in the left at 8 DPI. Satellite cells surrounding degenerative ganglion cells tended to be larger and more numerous than those surrounding morphologically intact and uninfected neurons in ganglia of the control mice. At 8 DPI, mild to moderate inflammatory cell infiltrates composed of lymphocytes, plasma cells and macrophages were observed in the right dorsal root ganglia (Fig. 2). In addition, significant axonal swelling, vacuoles and fragmentation with inflammatory cell infiltrates were observed in the right spinal dorsal root fibers (Fig. 3) and areas of the fasciculus gracilis in the spinal cord. The special staining (LFB) and immunohistochemical patterns of the NF were weaker in the spinal dorsal root areas than in the ventral motor spinal fibers (Fig. 4a and 4b). At 11 DPI, the majority of degenerative ganglion cells disappeared, while inflammatory cells significantly increased in the right side. In the ventral horn (motor neurons) and ventral spinal fibers, no morphological changes were observed throughout the experimental period.

No pathological changes were observed in the brain at 5 DPI. However, at 8 DPI, a small number of pyramidal neurons of the cerebral cortex showed nuclear pyknosis, karyorrhexis and cytoplasmic shrinkage, and the number of inflammatory cells was slightly higher in the leptomeninges and around blood vessels.

Immunohistochemical findings

Viral antigens were detected in the cytoplasm of the surae muscle of right triceps at 3 DPI (all 5 mice). Viral antigen showed a diffuse and granular pattern in the cytoplasm (Fig. 5). On the other hand, the viral antigen was not detected in muscles showing hyaline degeneration and inflammatory cells.

In the spinal cord, viral antigen-positive cells were initially detected in right lumbosacral dorsal root ganglion cells (Fig. 6a and 6b) (all 5 mice), right lumbosacral spinal cord dorsal horns (all 5 mice), lateral horns (4 of 5 mice) and ventral horns (2 of 5 mice) at 5 DPI. Most of viral antigen-positive cells in right lumbosacral dorsal root ganglia were consistent with ganglion cells that showed morphologically degenerative necrosis.

In the brain, viral antigens were found in the neurons of the left red nuclei of the midbrain (2 of 5), left M1 motor area of the cerebral cortex (2 of 5) and both sides of the medulla oblongata (3 of 5) at 5 DPI. At 8 DPI, the viral antigen-positive ganglion cells were observed in opposite sides of the spinal cord. Interestingly, viral antigen-positive cell numbers decreased in the right lumbosacral spinal cord at 8 DPI, and the cells completely disappeared at 11 DPI (Fig. 7a and 7b) (4 of 5 mice). Distribution of the rabies virus (1088) antigens in the surae muscles of the right triceps, lumbosacral dorsal root ganglia, spinal cord and brain at 3, 5, 8 and 11 DPI are summarized in Table 1.

At 8 DPI, few CD3-positive T lymphocytes appeared in the brain and spinal cord in the dorsal root spinal ganglia, leptomeninges, blood vessels and ventricles. At 11 DPI, the number of CD3-positive T lymphocytes significantly increased, and the cells scattered throughout the parenchyma of the brain (Fig. 8), spinal cord and dorsal root spinal ganglia, particularly around blood vessels. On the other hand, CD20-positive cells were very few in number throughout the experiment. Immunohistochemistry for Iba1 revealed enhanced reactivity around viral antigen-positive cells after 5 DPI in the spinal cord and right dorsal root spinal ganglia (Fig. 9). At 8 DPI, Iba1 positive cells altered their morphology from small rod-shaped cells to ramified or amoeboid cells and scattered throughout the CNS (Fig. 10). GFAP-positive cell numbers increased after 8 DPI and were mainly observed under the leptomeninges of the brain and spinal cord, around ventricles and the central canal.

TUNEL assays

From 8 DPI, a few TUNEL-positive cells appeared in pyramidal neurons of the cerebral cortex and in Purkinje and cerebellar

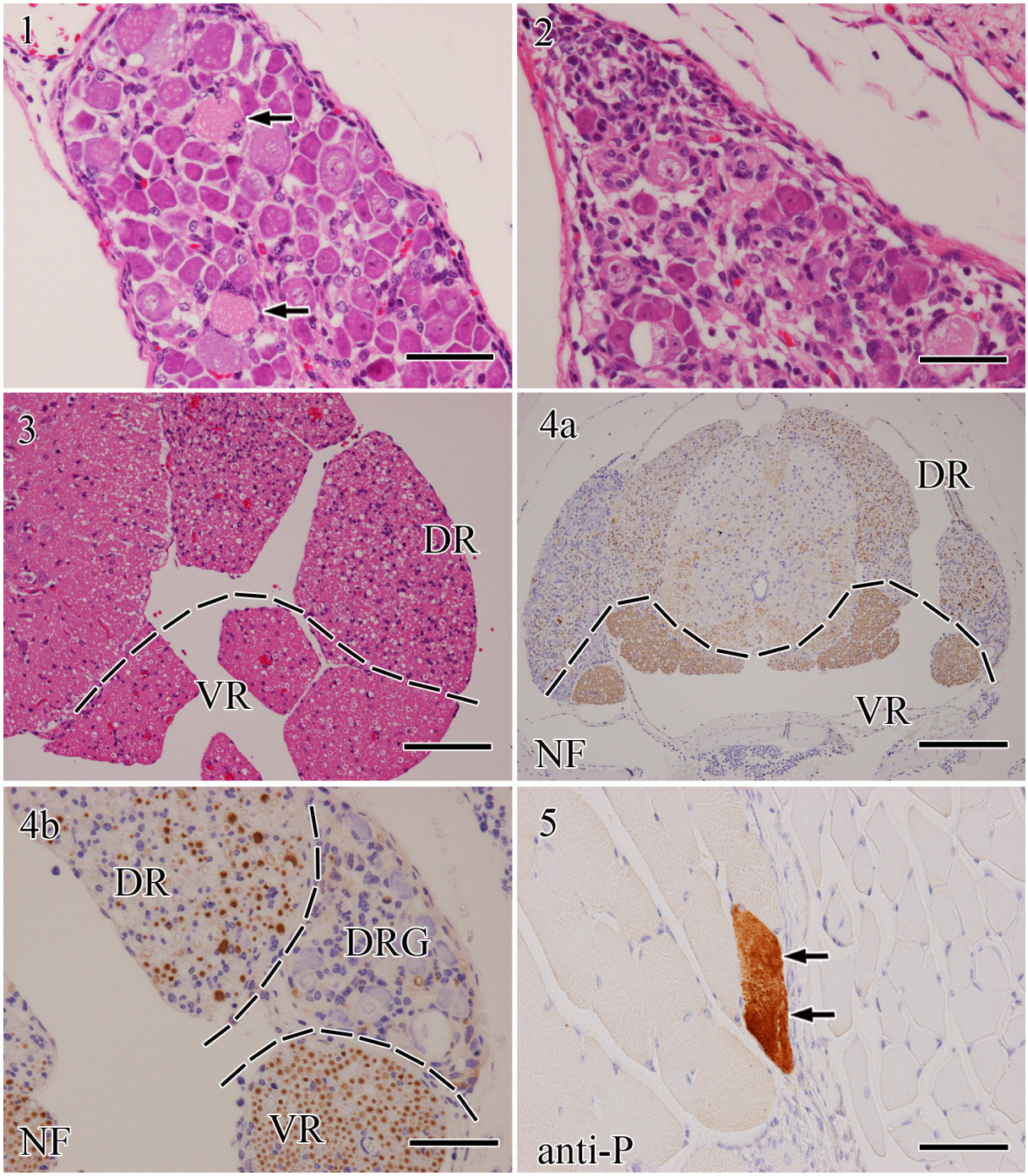

Fig. 1. Dorsal root ganglion at 5 DPI. Two dorsal root ganglion cells (arrows) show cytoplasmic chromatolysis. Hematoxylin-eosin staining. Bar=50 μm.

Fig. 2. Dorsal root ganglion at 8 DPI. Many mononuclear inflammatory cells and neurophagia seen in the dorsal root ganglion. Hematoxylin-eosin staining. Bar=50 μm.

Fig. 3. Dorsal and ventral root spinal fibers at 8 DPI. Infiltration of many mononuclear inflammatory cells and vacuolation are seen in the dorsal root spinal fiber, while no morphological changes are observed in the ventral root spinal fiber. DR: dorsal root spinal fiber, VR: ventral root spinal fiber. Hematoxylin-eosin staining. Bar=100 μm.

Fig. 4. Dorsal and ventral root spinal fibers at 8 DPI. Immunostaining intensity for neurofilament (NF) decreased in the dorsal root spinal fiber compared to the ventral root spinal fiber (4a, low magnification). The number of axons decreased, and some are enlarged compared to those in the ventral root spinal ganglion (4b, high magnification). DR: dorsal root spinal fiber, VR: ventral root spinal fiber. Immunohistochemistry. Bar=200 μm (4a), 500 μm (4b).

Fig. 5. Muscle at 3 DPI. Focal viral antigen-positive findings (arrows) are observed in the cytoplasm of muscle fibers. Immunohistochemistry. Bar=50 μm.

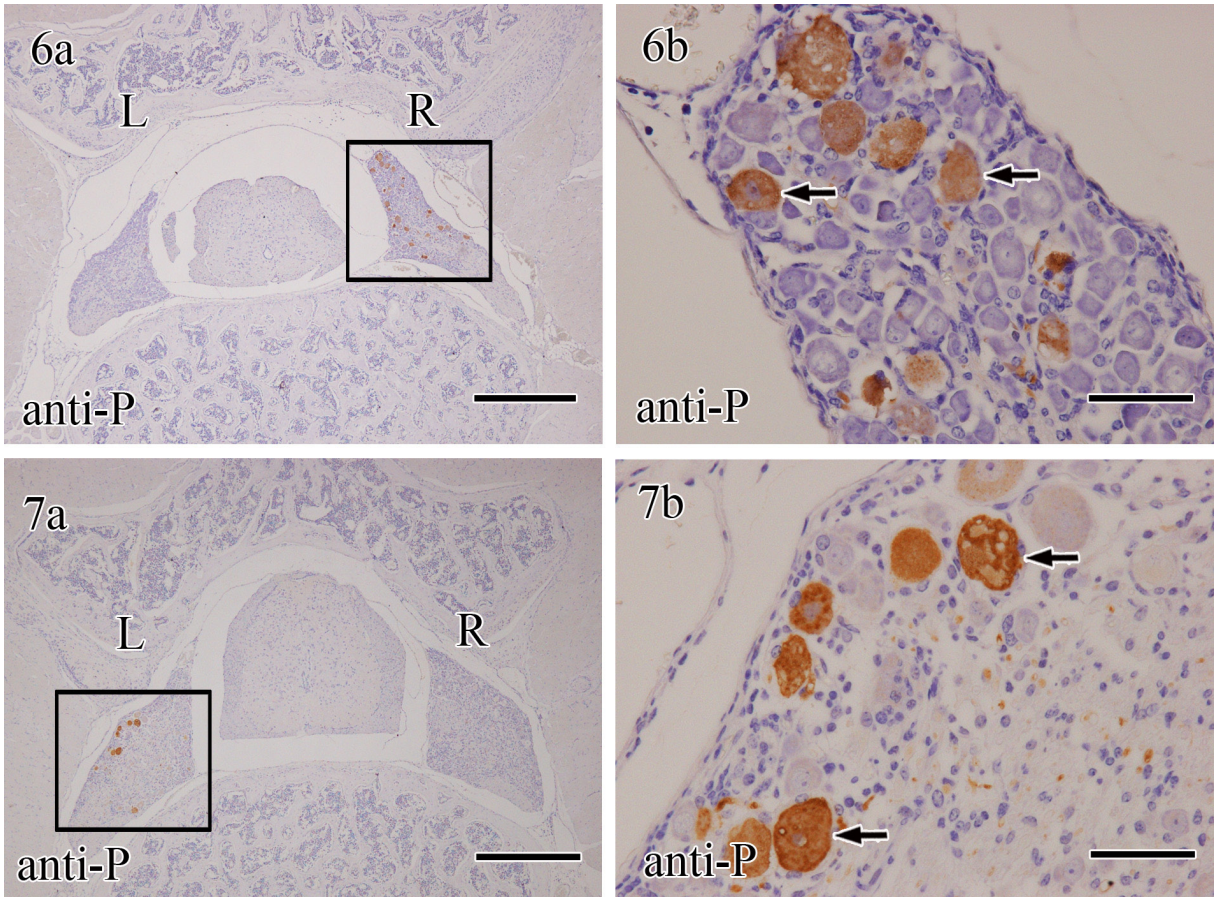

Fig. 6. Spinal cord and dorsal root ganglion at 5 DPI. Viral antigen-positive cells (encircled area and arrows) are only observed in the right dorsal root ganglion (6a, low magnification, 6b, high magnification). L: left, R: right. Immunohistochemistry. Bar=500 μm (6a), 50 μm (6b).

Fig. 7. Spinal cord and dorsal root ganglion at 11 DPI. Viral antigen-positive cells (encircled area and arrows) are only observed in the left dorsal root ganglion (7a, low magnification, 7b, high magnification). L: left, R: right. Immunohistochemistry. Bar=500 μm (7a), 50 μm (7b).

Table 1. Distribution of rabies virus (1088) antigens in the right triceps surae muscle, dorsal root ganglia, spinal cord and brain at 3, 5, 8 and 11 DPI

Days	Muscle	Lumbosacral DRG	Lumbosacral spinal cord			Brain			
			DH	LH	VH	RN	M1	S1	VPL
3d	0/5[a)]	0/0	0/0	0/0	0/0	0/0	0/0	0/0	0/0
5d	NT	0/5	0/5	1/4	0/2	2/0	2/0	0/0	0/0
8d	NT	5/4	4/4	4/4	3/3	5/5	5/5	5/5	5/5
11d	NT	3/1	3/3	3/3	0/0	5/5	5/5	5/5	5/5

Results expressed as the number of mice with positive staining for rabies virus antigen among each 5 mice used in experiment at the time point. a) left side/right side, DRG: dorsal root ganglion, DH: dorsal horn, LH: lateral horn, VH: ventral horn of spinal cord, RN: red nucleus, M1: cerebral cortex motor area, S1: cerebral cortex sensory area, VPL: ventral posterolateral thalamic nucleus, NT: no tested.

granular layer cells of the cerebellum. Lymphocytes in the leptomeningeal and perivascular areas of the brain (Fig. 11) and spinal cord were also TUNEL positive. In contrast, neurons of the spinal cord and dorsal root ganglion cells were not positive for TUNEL throughout the experimental period.

Ultrastructural findings

Virus particles were found in cell margins and interspersed among organelles of the perikaryon, especially in the rough endoplasmic reticulum (Nissl bodies) of the dorsal root spinal ganglion cells (Fig. 12). In ganglion cells infected with the virus, accumulation of Nissl bodies, a dark appearance, shrunken nuclei, irregular bundles of fine fibers and cytoplasmic vacuolization

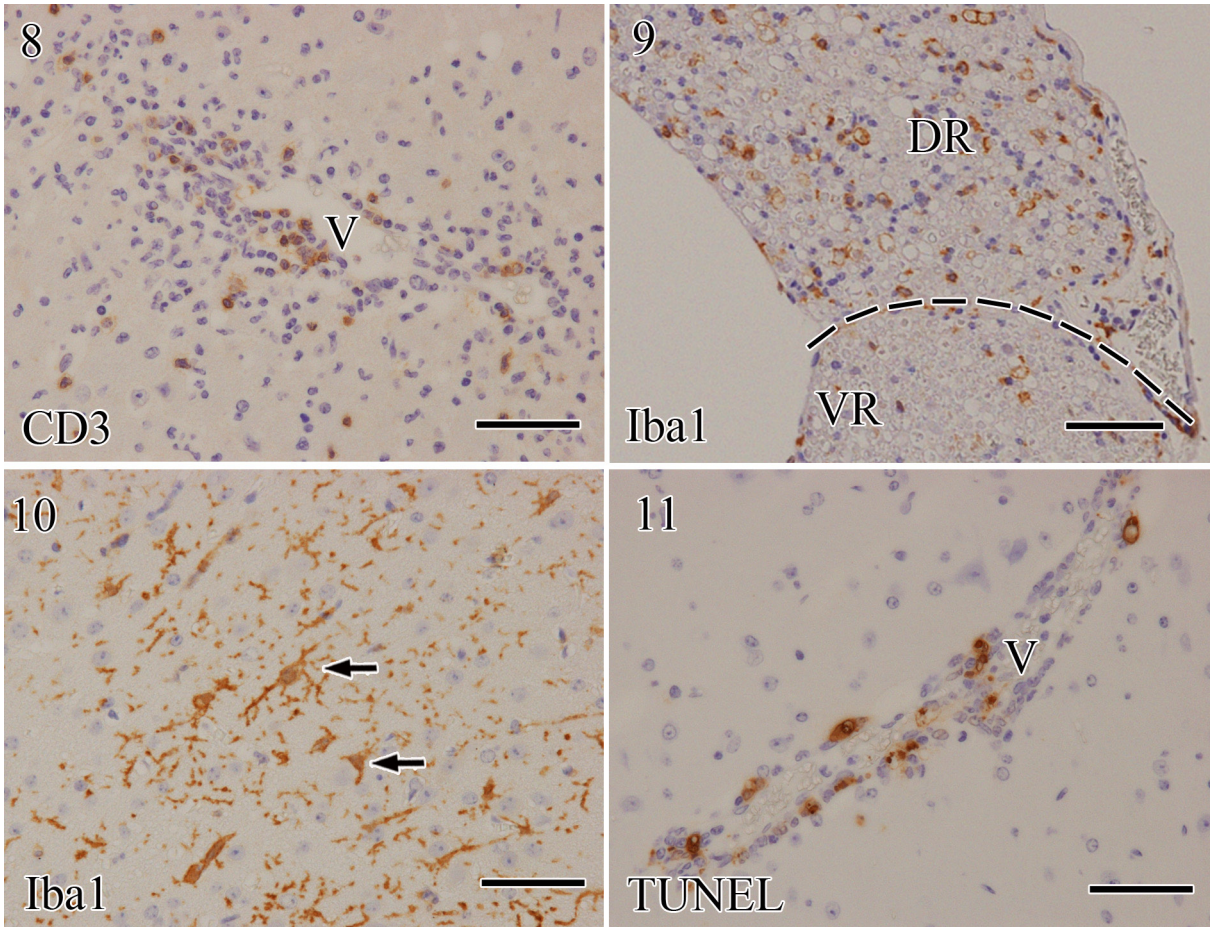

Fig. 8. Brain at 11 DPI. Many inflammatory cells around the small vein are positive for CD3. V: vein. Immunohistochemistry. Bar=50 μm.

Fig. 9. Dorsal and ventral root spinal fibers at 8 DPI. Iba1 positive cells mainly observed in the dorsal root spinal fibers. DR: dorsal root spinal fiber, VR: ventral root spinal fiber. Immunohistochemistry. Bar=50 μm.

Fig. 10. Brain at 8 DPI. Microglial cells are positive for Iba1 and changed their morphology to amoeboid shapes (arrows). Immunohistochemistry. Bar=50 μm.

Fig. 11. Brain at 8 DPI. TUNEL-positive cells are observed around the small vein. V: vein. TUNEL assay. Bar=50 μm.

constituted the cytopathological changes observed. Aggregation of swollen mitochondria, containing single membranous material and various sized vacuoles was observed in the myelinated axon of dorsal root fibers (Fig. 13).

DISCUSSION

In the present study, infiltration of inflammatory cells into right hindlimb muscles, at the site of inoculation, was observed at 3 DPI and persisted until the terminal stages of infection. The virus antigen was first detected in the hindlimb muscle fibers at 3 DPI prior to detection in the dorsal root ganglia and spinal cord at 5 DPI. In the pathogenesis of rabies, the muscle has been known to play an important role; however, it is unclear whether infection of muscle fibers is an essential step for access into the peripheral nervous system. In striped skunk, inoculated with a Canadian isolate of street rabies virus and prior to the development of clinical signs, viral antigen and genomic RNA were observed to be frequently present in the inoculated muscle, but not in the spinal ganglia or spinal cord [7]. In contrast, Coulon *et al*. [8] and Shankar *et al*. [28] did not find any evidence of viral replication in the muscle of mice inoculated with the challenge virus standard (CVS) strain and concluded that CVS strains can penetrate directly into peripheral nerves without replicating in the muscle during the short incubation period. Our results supported the results of the former study, suggesting that viral replication in muscle fibers during the incubation period is necessary for retrograde spread of the virus from muscle fibers to spinal cords in the 1088 strain.

Dorsal root spinal ganglion cells are pseudo-unipolar primary sensory neurons with a single axon that divides into peripheral and central branches. Ganglion cells are crucial in the initial events of rabies infection, since they can facilitate viral entrance into the CNS. In general, street rabies virus strains have lesser tendency to induce cytopathic changes in neurons than that of fixed rabies virus strains, which could be attributed to their neuroadaptation due to serial passage in animal brains [25]. In the present

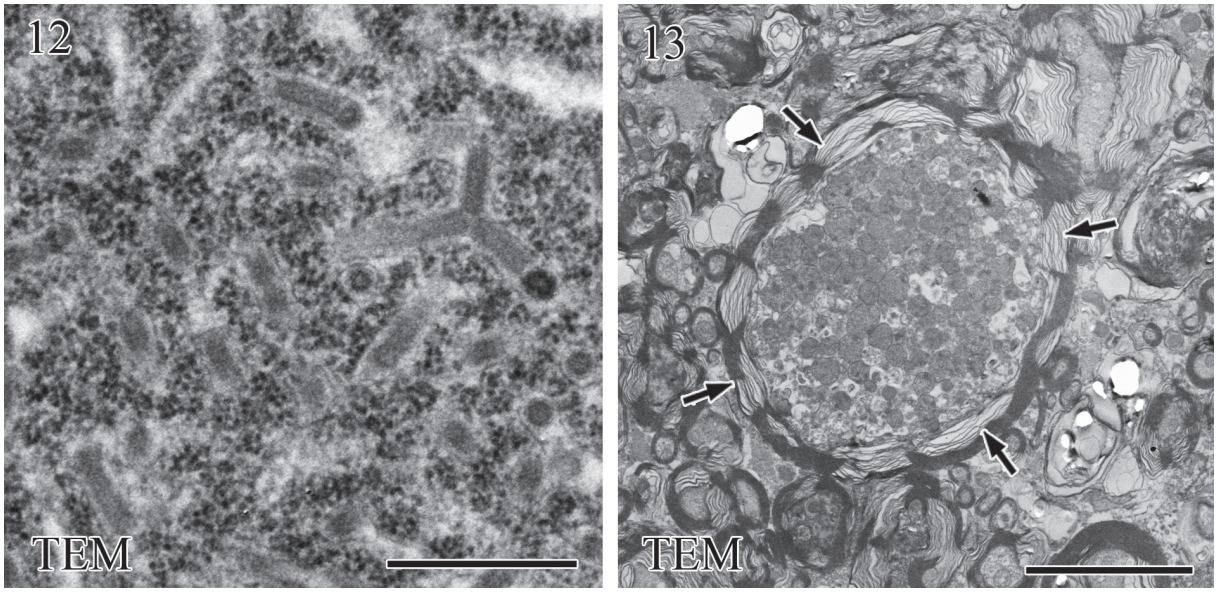

Fig. 12. Dorsal root ganglion at 8 DPI. Many virus particles are seen in the rough endoplasmic reticuluma (Nissl bodies). Electron microscopy. Bar=500 nm.

Fig. 13. Dorsal root spinal fibers at 8 DPI. Aggregation of swollen mitochondria containing single membranous material and various sized vacuoles is observed in the myelinated axon (arrows). Electron microscopy. Bar=5 μm.

study, degenerative necrosis of ganglion cells and their nerves in the right dorsal root spinal ganglia were observed at 5 DPI. At this time point, inflammatory cell infiltrates were not observed. In addition, morphological findings of degenerative ganglion cells showed not typical apoptosis features, and the TUNEL assay which detects the presence of fragmented DNA was negative. These histopathological findings suggest that degenerative necrosis in the ganglion cells and their nerves is a result of direct neuronal injury due to virus infection. The results obtained in this study are similar to those reported in studies for sensory ganglia in humans [20, 33] and experimental infection in animals using peripheral routes of inoculation [22, 26].

In the present study, high numbers of inflammatory cells infiltrated into the right dorsal root ganglia along with the appearance of degenerative ganglion cells and electron microscopically axonal degeneration, such as mitochondrial swelling and vacuolar degeneration were observed from 8 DPI. Previously, Jackson *et al*. [14] reported that cultured dorsal root ganglion cells infected with the challenge virus standard-11 strain of rabies virus show axonal swellings and these degenerated axons show positive for oxidative stress marker (4-hydroxy-2-nonenal), indicating evidence of lipid peroxidation associated with oxidative stress. So, they postulated that rabies virus infection likely induces mitochondrial dysfunction, resulting in oxidative stress and degenerative changes involving neuronal processes. In the present study, it is unknown whether oxidative stress has occurred in axons of infected mouse, and therefore further studies are needed using an *in vivo* model of street rabies virus.

In the present study, viral antigens in the CNS were first detected in the right lumbosacral dorsal root ganglia, right lumbosacral spinal cord, left red nucleus and left cerebral cortex (M1 areas) at 5 DPI. These findings suggested the possibility that the 1088 viral strain ascended the cell body of the primary neuron of the spinal dorsal root ganglia and ventral horn via sensory nerve fibers and motor nerve fibers, respectively, and then, the virus in the spinal ventral horn rapidly moved to the red nucleus and the cerebral cortex (M1 areas) using the descending spinal tract (rubrospinal tract and corticospinal tract) (Fig. 14).

Interestingly, after 8 DPI, viral antigen-positive ganglion cells were observed to gradually decrease and disappear from the right dorsal root ganglia, while CD3-positive cells were observed to increase. The CD3 molecule is a surface marker of T lymphocytes which play an important role in cellular immunity by blocking viral spread and clearing rabies virus from the CNS [3, 12]. Therefore, in the present study, we assumed that T lymphocyte-mediated immune response played an important role in the clearance of rabies virus from the spinal dorsal root ganglia.

Microglial cells represent 5–15% of brain cells and are intracerebral resident macrophages [23] that alter their morphological forms between ramified (resting) and amoeboid (activated) types after CNS injury [24, 30]. Activated microglial cells produce various proinflammatory cytokines and chemokines, such as interleukin-1, CXCL10, tumor necrosis factor alpha, matrix metalloproteinases, superoxide and nitric oxide [24], which mediate nerve cell death both directly and indirectly via the induction of nitric oxide and free radicals [13] and nitric oxide-induced cytotoxicity via oxidative injury, resulting in immunosuppression and immunopathology [1]. Matrix metalloproteinases are secretory products of activated microglial cells which can contribute to the breakdown of the blood-brain barrier, leukocyte emigration into the nervous system and tissue destruction [24]. Interleukin-1 and tumor necrosis factor alpha released by microglial cells play an important role in coordinating the inflammatory response associated with rabies encephalopathy [18]. In this study, the number of Iba1 antibody-positive cells increased significantly from 8 DPI, and their morphology changed from a ramified

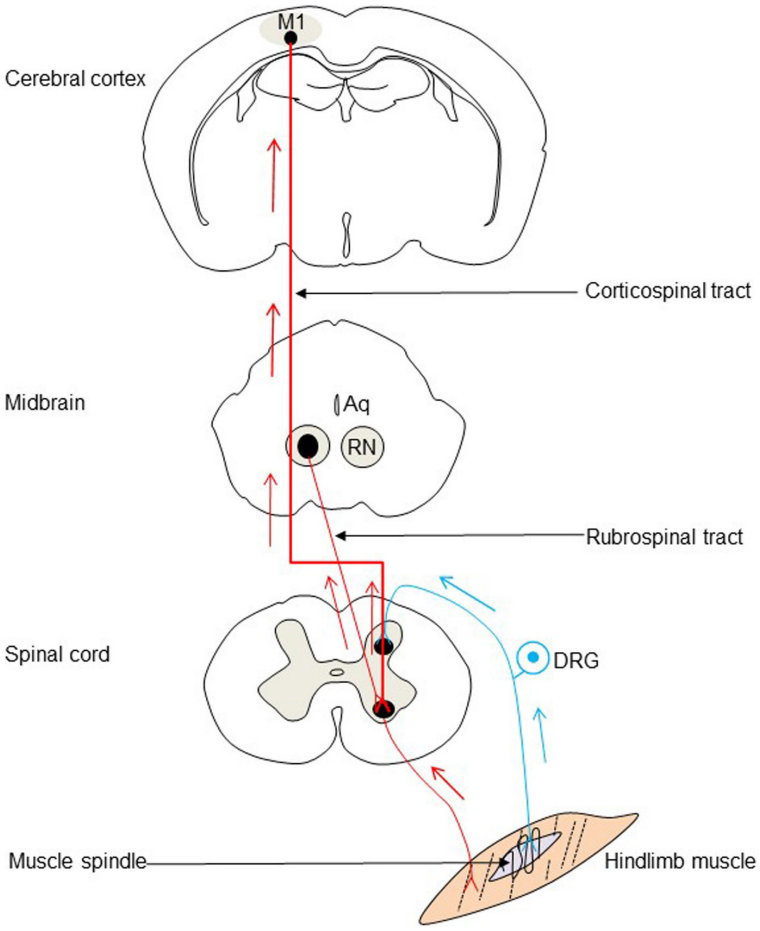

Fig. 14. Possible routes of street rabies virus (1088 strain) invasion into the CNS in the present study. 1088 strain invades the spinal cord using sensory nerves (blue line) and motor nerves (red line) after proliferating in the hindlimb muscles including muscle spindle, and then, the virus rapidly moves to the red nucleus and the cerebral cortex (M1 areas) using the descending spinal tracts (rubrospinal tract and corticospinal tract). Aq: aqueduct, DRG: dorsal root ganglion, M1: cerebral cortex (M1) area, RN: red nucleus.

to an amoeboid form in areas where many virus-infected and necrotic cells were present. Therefore, it was assumed that activated microglial cells and their inflammatory cytokines contribute to inflammation and neuronal necrosis in the spinal cord and brain.

Although the morphological changes of astroglial cells were not clear in HE section, GFAP positive cells increased in the spinal cord at 8 DPI and were observed under leptomeninges and around ventricles. Astroglial cells have essential roles to protect neuronal tissues and to control inflammatory reaction by producing cytokines and neurotrophic factors after CNS injury [9]. However, the role of the cells in the present experimental study is still unresolved.

In the case of rabies, strong evidence of apoptosis was found in both cultured cells [21] and neurons in experimental mouse rabies models infected by intracerebral inoculation of fixed rabies virus strains [22], while neuronal apoptosis has not been prominent in natural rabies animals. In the brain of rabid dogs, the viral antigen bearing neurons or glial cells do not undergo apoptosis, while inflammatory cells, microglial cells, endothelial cells and macrophages present apoptotic changes [31, 32]. In the present study, a few virus-infected nerve cells in the pyramidal layer of cerebral cortex, cerebellar Purkinje cells and virus uninfected inflammatory cells were positive for TUNEL assay. On the other hand, virus-infected dorsal root ganglion cells, spinal neurons and most nerve cells in other areas of brain were negative for TUNEL. These aspects are partially in accordance with those of previously reported papers [22, 26]. However, the role of apoptosis in natural rabies pathogenesis is still controversial, and therefore, further studies are needed on this aspect of the disease.

In summary, *dd*Y mice that were inoculated intramuscularly with the street rabies virus strain 1088, isolated from a woodchuck, exhibit paralytic signs and the pathological changes are more severe in the dorsal root ganglion neurons and their nerve fibers than in the nerve cells of the brain and spinal cord. Therefore, we could conclude that the clinical signs (paralysis) in rabies infection were possibly because of the selective susceptibility of dorsal root ganglion neurons and their nerve fibers in mice infected with 1088 strain.

ACKNOWLEDGMENTS. This work was supported by a Grant-in-Aid for Scientific Research from the Japan Society for the Promotion of Science (KAKENHI No. 26450410) and a Grant for Scientific Research from the KITASATO University, Heiwa Nakajima Foundation, and the Japan Agency for Medical Research and Development (AMED).

REFERENCES

1. Akaike, T. and Maeda, H. 2000. Nitric oxide and virus infection. *Immunology* **101**: 300–308. [Medline] [CrossRef]
2. Baer, G. M. 2007. The history of rabies. pp. 1–22. *In*: Rabies, 2nd ed. (Jackson, A. C. and Wunner, W. H. eds.), Academic Press, San Diego.
3. Baloul, L. and Lafon, M. 2003. Apoptosis and rabies virus neuroinvasion. *Biochimie* **85**: 777–788. [Medline] [CrossRef]
4. Boonsriroj, H., Manalo, D. L., Kimitsuki, K., Shimatsu, T., Shiwa, N., Shinozaki, H., Takahashi, Y., Tanaka, N., Inoue, S. and Park, C. H. 2016. A pathological study of the salivary glands of rabid dogs in the Philippines. *J. Vet. Med. Sci.* **78**: 35–42. [Medline] [CrossRef]
5. Charlton, K. M. 1984. Rabies: spongiform lesions in the brain. *Acta Neuropathol.* **63**: 198–202. [Medline] [CrossRef]
6. Charlton, K. M., Casey, G. A., Webster, W. A. and Bundza, A. 1987. Experimental rabies in skunks and foxes. Pathogenesis of the spongiform lesions. *Lab. Invest.* **57**: 634–645. [Medline]
7. Charlton, K. M., Nadin-Davis, S., Casey, G. A. and Wandeler, A. I. 1997. The long incubation period in rabies: delayed progression of infection in muscle at the site of exposure. *Acta Neuropathol.* **94**: 73–77. [Medline] [CrossRef]
8. Coulon, P., Bras, H. and Vinay, L. 2011. Characterization of last-order premotor interneurons by transneuronal tracing with rabies virus in the neonatal mouse spinal cord. *J. Comp. Neurol.* **519**: 3470–3487. [Medline] [CrossRef]
9. Farina, C., Aloisi, F. and Meinl, E. 2007. Astrocytes are active players in cerebral innate immunity. *Trends Immunol.* **28**: 138–145. [Medline] [CrossRef]
10. Hemachudha, T., Wacharapluesadee, S., Laothamatas, J. and Wilde, H. 2006. Rabies. *Curr. Neurol. Neurosci. Rep.* **6**: 460–468. [Medline] [CrossRef]
11. Hemachudha, T., Ugolini, G., Wacharapluesadee, S., Sungkarat, W., Shuangshoti, S. and Laothamatas, J. 2013. Human rabies: neuropathogenesis, diagnosis, and management. *Lancet Neurol.* **12**: 498–513. [Medline] [CrossRef]
12. Hooper, D. C., Morimoto, K., Bette, M., Weihe, E., Koprowski, H. and Dietzschold, B. 1998. Collaboration of antibody and inflammation in clearance of rabies virus from the central nervous system. *J. Virol.* **72**: 3711–3719. [Medline]
13. Hu, S., Peterson, P. K. and Chao, C. C. 1997. Cytokine-mediated neuronal apoptosis. *Neurochem. Int.* **30**: 427–431. [Medline] [CrossRef]
14. Jackson, A. C., Kammouni, W., Zherebitskaya, E. and Fernyhough, P. 2010. Role of oxidative stress in rabies virus infection of adult mouse dorsal root ganglion neurons. *J. Virol.* **84**: 4697–4705. [Medline] [CrossRef]
15. Knobel, D. L., Cleaveland, S., Coleman, P. G., Fèvre, E. M., Meltzer, M. I., Miranda, M. E., Shaw, A., Zinsstag, J. and Meslin, F. X. 2005. Re-evaluating the burden of rabies in Africa and Asia. *Bull. World Health Organ.* **83**: 360–368. [Medline]
16. Kojima, D., Park, C. H., Satoh, Y., Inoue, S., Noguchi, A. and Oyamada, T. 2009. Pathology of the spinal cord of C57BL/6J mice infected with rabies virus (CVS-11 strain). *J. Vet. Med. Sci.* **71**: 319–324. [Medline] [CrossRef]
17. Lépine, P. 1938. On the evolution of fixed strains of rabies virus. *J. Hyg. (Lond.)* **38**: 180–184. [Medline] [CrossRef]
18. Marquette, C., Van Dam, A. M., Ceccaldi, P. E., Weber, P., Haour, F. and Tsiang, H. 1996. Induction of immunoreactive interleukin-1 beta and tumor necrosis factor-alpha in the brains of rabies virus infected rats. *J. Neuroimmunol.* **68**: 45–51. [Medline] [CrossRef]
19. Mifune, K., Makino, Y. and Mannen, K. 1979. Susceptibility of various cell lines to rabies virus. Japan. *J. Trop. Med. Hyg.* **7**: 201–208. [CrossRef]
20. Mitrabhakdi, E., Shuangshoti, S., Wannakrairot, P., Lewis, R. A., Susuki, K., Laothamatas, J. and Hemachudha, T. 2005. Difference in neuropathogenetic mechanisms in human furious and paralytic rabies. *J. Neurol. Sci.* **238**: 3–10. [Medline] [CrossRef]
21. Morimoto, K., Hooper, D. C., Spitsin, S., Koprowski, H. and Dietzschold, B. 1999. Pathogenicity of different rabies virus variants inversely correlates with apoptosis and rabies virus glycoprotein expression in infected primary neuron cultures. *J. Virol.* **73**: 510–518. [Medline]
22. Park, C. H., Kondo, M., Inoue, S., Noguchi, A., Oyamada, T., Yoshikawa, H. and Yamada, A. 2006. The histopathogenesis of paralytic rabies in six-week-old C57BL/6J mice following inoculation of the CVS-11 strain into the right triceps surae muscle. *J. Vet. Med. Sci.* **68**: 589–595. [Medline] [CrossRef]
23. Perry, V. H., Hume, D. A. and Gordon, S. 1985. Immunohistochemical localization of macrophages and microglia in the adult and developing mouse brain. *Neuroscience* **15**: 313–326. [Medline] [CrossRef]
24. Rock, R. B., Gekker, G., Hu, S., Sheng, W. S., Cheeran, M., Lokensgard, J. R. and Peterson, P. K. 2004. Role of microglia in central nervous system infections. *Clin. Microbiol. Rev.* **17**: 942–964. [Medline] [CrossRef]
25. Rossiter, J. P. and Jackson, A. C. 2007. Pathology. pp. 383–409. *In*: Rabies, 2nd ed. (Jackson, A. C. and Wunner, W. H. eds.), Academic Press, San Diego.
26. Rossiter, J. P., Hsu, L. and Jackson, A. C. 2009. Selective vulnerability of dorsal root ganglia neurons in experimental rabies after peripheral inoculation of CVS-11 in adult mice. *Acta Neuropathol.* **118**: 249–259. [Medline] [CrossRef]
27. Roy, A. and Hooper, D. C. 2007. Lethal silver-haired bat rabies virus infection can be prevented by opening the blood-brain barrier. *J. Virol.* **81**: 7993–7998. [Medline] [CrossRef]
28. Shankar, V., Dietzschold, B. and Koprowski, H. 1991. Direct entry of rabies virus into the central nervous system without prior local replication. *J. Virol.* **65**: 2736–2738. [Medline]
29. Shimatsu, T., Shinozaki, H., Kimitsuki, K., Shiwa, N., Manalo, D. L., Perez, R. C., Dilig, J. E., Yamada, K., Boonsriroj, H., Inoue, S. and Park, C. H. 2016. Localization of the rabies virus antigen in Merkel cells in the follicle-sinus complexes of muzzle skins of rabid dogs. *J. Virol. Methods* **237**: 40–46. [Medline] [CrossRef]
30. Streit, W. J. 2002. Microglia as neuroprotective, immunocompetent cells of the CNS. *Glia* **40**: 133–139. [Medline] [CrossRef]
31. Suja, M. S., Mahadevan, A., Madhusudana, S. N. and Shankar, S. K. 2011. Role of apoptosis in rabies viral encephalitis: a comparative study in mice, canine, and human brain with a review of literature. *Pathol. Res. Int.* **2011**: 374286. [Medline] [CrossRef]
32. Suja, M. S., Mahadevan, A., Madhusudhana, S. N., Vijayasarathi, S. K. and Shankar, S. K. 2009. Neuroanatomical mapping of rabies nucleocapsid viral antigen distribution and apoptosis in pathogenesis in street dog rabies--an immunohistochemical study. *Clin. Neuropathol.* **28**: 113–124. [Medline] [CrossRef]
33. Tangchai, P. and Vejjajiva, A. 1971. Pathology of the peripheral nervous system in human rabies. A study of nine autopsy cases. *Brain* **94**: 299–306. [Medline] [CrossRef]
34. Yamada, K., Park, C. H., Noguchi, K., Kojima, D., Kubo, T., Komiya, N., Matsumoto, T., Mitui, M. T., Ahmed, K., Morimoto, K., Inoue, S. and Nishizono, A. 2012. Serial passage of a street rabies virus in mouse neuroblastoma cells resulted in attenuation: potential role of the additional N-glycosylation of a viral glycoprotein in the reduced pathogenicity of street rabies virus. *Virus Res.* **165**: 34–45. [Medline] [CrossRef]
35. Yan, X., Prosniak, M., Curtis, M. T., Weiss, M. L., Faber, M., Dietzschold, B. and Fu, Z. F. 2001. Silver-haired bat rabies virus variant does not induce apoptosis in the brain of experimentally infected mice. *J. Neurovirol.* **7**: 518–527. [Medline] [CrossRef]